터널과 지하공간, 한국암반공학회
Vol. 10, 2000, pp. 301~308

TUNNEL & UNDERGROUND Vol. 10, 2000, pp. 301-308
J. of Korean Society for Rock Mech.

암석내의 균열전파에 따른 유효탄성계수의 변화

신종진[1] · 전석원[2]

Changes of Effective Elastic Moduli due to Crack Growth in Rock

Jong-Jin Shin and Seok-Won Jeon

ABSTRACT Non-linear behavior of rock under compression can be predicted by a crack model. Crack growth in rock renders rock anisotropic. The degree of anisotropy is explained in terms of elastic moduli as a function of load level. In this study, we calculate the changes of elastic moduli due to crack growth numerically by using a crack model and compare these values with experimental results obtained from the measurement of ultrasonic wave velocities. Image processing technique is used to obtain the initial crack information needed for the numerical calculation of elastic moduli.

Key words : effective elastic moduli, sliding crack model, transverse isotropy, ultrasonic wave velocity

초 록 : 균열모형을 이용하여 압축 하중하에 있는 암석의 비선형 거동을 예측하는 것은 가능하다. 암석내의 균열의 성장은 암석의 이방성을 가져오며, 이러한 이방성의 정도는 탄성계수의 변화로 표현될 수 있다. 본 연구에서는 균열의 성장에 따른 탄성계수의 변화를 이론적인 균열모형을 통해 예측하고, 이를 탄성파 속도 시험을 통해 구한 탄성계수와의 비교를 수행하였다. 또한, 균열모형에 사용되는 초기 암석내 존재하는 균열에 대한 정보는 암석표면의 이미지를 분석하여 구하였다.

핵심어 : 유효탄성계수, 활주균열모형, 횡등방성, 탄성파 속도

1. Introduction

Cracks in rock have brought about the engineering concern because the propagation of initial cracks is known to be the major reason for deformation and failure of rock. Since many engineering hazards arise from the results of the propagation of these cracks, understanding the mechanism of crack growth and the behavior of rock is necessary in preventing future accidents.

Under a deviatoric compressive stress field, cracks grow, interact and coalesce in response to the locally induced tensile stress (Kemeny & Cook, 1987, 1991; Kemeny, 1993; Shea & Hanson, 1998). The pre-existing and stress-induced cracks grow in either extensile or shear mode depending on whether the crack surfaces close to the crack tip move perpendicular or parallel to the instantaneous plane of propagation, respectively (Kranz, 1983). However, cracks in a brittle material tend to grow parallel to the maximum principal stress. This results in anisotropy, transverse isotropy in a two dimensional case, which has been described by crack models (Kemeny, 1993; Jeon, 1997).

Five independent elastic constants explaining the behavior of transversely isotropic rock can be numerically calculated from a proper crack model. And these values can also be determined from ultrasonic wave velocities. Much research has been done to describe the anisotropy using wave velocities (Jones & Wang, 1981; Lockner et al., 1977; Sayers et al., 1990, 1995; Watanabe & Sassa, 1995; Wu et al., 1991). These studies show that ultrasonic wave velocities change after the growth of cracks. From the results, we know that measuring wave velocities is a good way to assess the degree of crack propagation in rock.

In this study, changes of elastic moduli are predicted

1)정회원, 서울대학교 지구환경시스템공학부
2)정회원, 서울대학교 지구환경시스템공학부 조교수
접수일 : 2000년 7월 31일
심사 완료일 : 2000년 8월 12일

by a crack model, in which the input parameters such as crack density, crack length and crack orientation are obtained from image processing technique. At the same time, changes of elastic moduli are determined experimentally by measuring the ultrasonic wave velocities.

2. Theoretical Background

Arbitrary oriented cracks in rock under loading tend to grow parallel to the maximum principal stress, which makes the rock have different characteristics or physical properties from those under the initially unstressed condition. Even isotropic rock changes into anisotropic rock due to the results of crack growth in rock. To predict the behavior of the rock with growing cracks, sliding crack model is used in this study, which was successfully used by Kemeny (1993) and Jeon (1997) to explain the non-linear stress-strain behavior of rock. Fig. 1 shows that a single crack under the compressive load grows toward the direction of the maximum principal stress, σ_1, which becomes a sliding crack.

Stress intensity factor of a sliding crack has the following form for an applied uniaxial stress σ_y:

$$K_I = \frac{2l_o\tau^* c}{\sqrt{\pi l}} = \frac{2l_o(sc-\mu c^2)c}{\sqrt{\pi l}} \tag{1}$$

where K_I = mode I stress intensity factor, $2l_o$ = initial crack length, $2l$ = changed crack length, τ^* = effective shear stress on the crack surface, μ = frictional coefficient, $s = \sin\theta$, $c = \cos\theta$ and θ = orientation of the crack measured from the horizon.

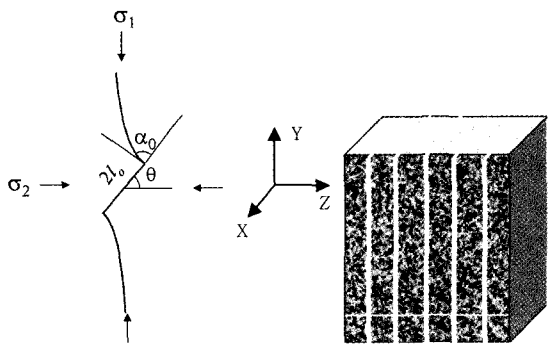

(a) A sliding crack (b) Transversely isotropy

Fig. 1. A sliding crack and transverse isotropy due to crack growth.

When $K_I = K_{IC}$, which is the fracture toughness for mode I, a sliding crack initiates growth. If the grown cracks are aligned parallel to the uniaxial loading direction, as is usual for the brittle materials, the rock containing many sliding cracks is rendered transversely isotropic with five independent elastic constants, especially in the two dimensional case (Fig. 1).

When unstressed initial rock is assumed to be the isotropic and elastic material, there is two independent elastic constants governing the material behavior, Youngs modulus E and Poissons ratio ν. After the onset of crack growth, however, five independent elastic constants or E_1, E_2, ν_1, ν_2 and G_2 are required to describe the behavior of the transverse isotropic material. And these five values are called "effective elastic moduli" in the sense that they change as the cracks grow and they represent the extent of the anisotropy.

Elastic constitutive relations for transverse isotropy are as follows:

$$\begin{bmatrix}\varepsilon_x\\ \varepsilon_y\\ \varepsilon_z\\ \gamma_{yz}\\ \gamma_{zx}\\ \gamma_{xy}\end{bmatrix} = \begin{bmatrix} 1/E_1 & -\nu_1/E_1 & -\nu_2/E_2 & 0 & 0 & 0\\ -\nu_1/E_1 & 1/E_1 & -\nu_2/E_2 & 0 & 0 & 0\\ -\nu_2/E_2 & -\nu_2/E_2 & 1/E_2 & 0 & 0 & 0\\ 0 & 0 & 0 & 1/G_2 & 0 & 0\\ 0 & 0 & 0 & 0 & 1/G_2 & 0\\ 0 & 0 & 0 & 0 & 0 & 1/G_1\end{bmatrix}\begin{bmatrix}\sigma_x\\ \sigma_y\\ \sigma_z\\ \tau_{yz}\\ \tau_{zx}\\ \tau_{xy}\end{bmatrix} \tag{2}$$

Here, Z is the axis of symmetry of transverse isotropy and XY plane is the plane of isotropy. E_1 and ν_1 are Young's modulus and Poisson's ratio in the plane of isotropy. E_2 and ν_2 are Young's modulus and Poisson's ratio in a direction normal to the plane of isotropy. G_2 is the shear modulus in planes normal to the plane of isotropy.

To derive five effective elastic moduli, the displacement of an elastic body containing cracks is required to determine by using Hooke's law for the elastic displacements and Castigliano's theorem for the crack-induced displacements. According to Castigliano's theorem, the component u_i of the displacement vector **u** in the direction of the load P_i is given as follows (Reismann & Pawlik, 1980; Sokolnikoff, 1956):

$$u_I = \frac{\partial u^*}{\partial p_i} \tag{3}$$

U* is the strain energy stored in the body. And the

energy release rate G has the following form as a function of three stress intensity factors, K_I, K_{II} and K_{III}:

$$G = \frac{K_I^2}{E'} + \frac{K_{II}^2}{E'} + \frac{K_{III}^2}{E}(1+\nu) \tag{4}$$

$$G = \frac{1}{2}\frac{\partial U^*}{\partial l} \tag{5}$$

By integrating G over the crack length l and using equations (3) and (4), the total displacements u_t of an elastic body containing cracks are obtained as a sum of the displacements of an elastic body u_e and the displacements due to the crack growth, as follows:

$$u_t = u_e + \frac{\partial}{\partial p}\left[\int_{l_0}^{l} 2G\,dl\right]$$
$$= u_e + \frac{\partial}{\partial p}\left[\int_{l_0}^{l} 2\left\{\frac{K_I^2}{E'} + \frac{K_{II}^2}{E'} + \frac{K_{III}^2}{E}(1+\nu)\right\}dl\right] \tag{6}$$

Thus, considering N cracks, the strain in the direction of the load, Y axis is calculated as follows:

$$\varepsilon_y = \frac{\sigma_y}{E}\left[1 + \frac{16}{\pi(vol)}\sum_{i=1}^{N} l_{oi}^2 (s_i c_i - \mu c_i^2)^2 c_i^2 \ln\frac{l_i}{l_{oi}}\right] \tag{7}$$

where (*vol*) = volume of the specimen containing N cracks and *i* denotes the *i*-th crack. Therefore, one of the effective elastic moduli, E_1 can be given as shown below:

$$E_1 = \frac{E}{\left[1 + \frac{16}{\pi(vol)}\sum_{i=1}^{N} l_{oi}^2 (s_i c_i - \mu c_i^2)^2 c_i^2 \ln\frac{l_i}{l_{oi}}\right]} \tag{8}$$

In the same manner, we can obtain the other effective elastic moduli.

$$E_2 = \frac{E}{\left[1 + \frac{2\pi}{\pi(vol)}\sum_{i=1}^{N} l_{oi}^2 \left\{\left(\frac{l_i}{l_{oi}}\right)^2 - 1\right\}\right]} \tag{9}$$

$$G_2 = \frac{G}{\left[1 + \frac{\pi}{(vol)(1+\nu)}\sum_{i=1}^{N} l_{oi}^2 \left\{\left(\frac{l_i}{l_{oi}}\right)^2 - 1\right\}\right]} \tag{10}$$

$$\nu_1 = \frac{\nu}{\left[1 + \frac{\pi}{\pi(vol)}\sum_{i=1}^{N} l_{oi}^2 (s_i c_i - \mu c_i^2)^2 c_i^2 \ln\frac{l_i}{l_{oi}}\right]} \tag{11}$$

$$\nu_2 = \frac{\left[\nu + \frac{8}{(vol)}\sum_{i=1}^{N} l_{oi}^2 (s_i c_i - \mu c_i^2) c_i \left(\frac{l_i}{l_{oi}} - 1\right)\right]}{\left[1 + \frac{16}{\pi(vol)}\sum_{i=1}^{N} l_{oi}^2 (s_i c_i - \mu c_i^2)^2 c_i^2 \ln\frac{l_i}{l_{oi}}\right]} \tag{12}$$

3. Initial Crack Information

Statistical data of the pre-existing cracks in rock are required to calculate effective elastic moduli according to crack growth. The possible ways to obtain these information about the initial cracks are creep test and compression test with resin injection for observing the distribution of crack length and crack orientation and the scanline survey, a procedure that involves the counting of the number of intersections that an array of parallel lines make with cracks in a plane section (Underwood, 1970). But the more accurate way for the crack information is to measure the crack length, the crack orientation and the number of cracks directly from the images such as video images or SEM (Scanning Electron Microscope) images. This method needs special care to prepare the rock section because of surface damages and cracking on the section that we want to examine.

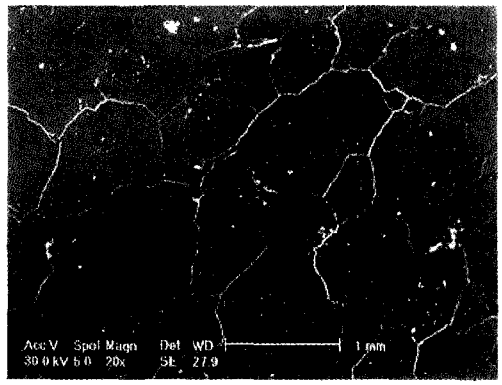

Fig. 2. SEM image of Yeosan marble with 256 grayscales.

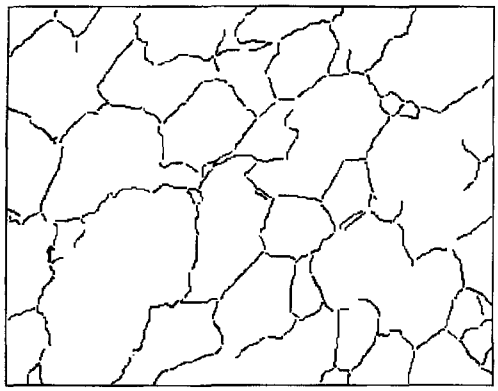

Fig. 3. Binary image of Yeosan marble.

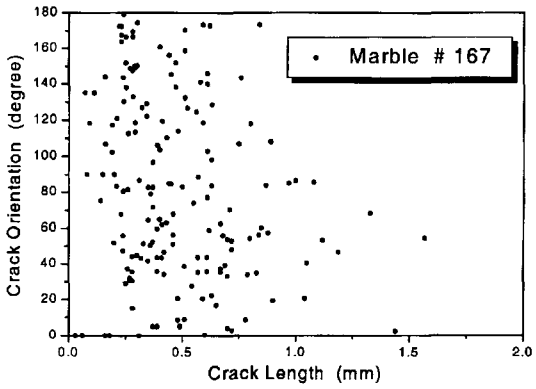

Fig. 4. Crack orientation vs. crack length.

SEM image of Yeosan marble shown in Fig. 2 is used for the direct measurement of crack data. NIH (US National Institute of Health) Image program enables us to process this digitized image with 256 grayscales. Thresholding, one of the menus on the program is used to segment an image into objects of interest, which is the cracks, and the background on the basis of gray level. Fig. 3 shows the binary image where only cracks are black with the white background. Finally, this binary image is used to obtain the crack information such as crack density, crack length and crack orientation.

The number of cracks observed in the image is 167 on the area of 14.08 mm^2 and the relation between crack length and crack orientation is shown in Fig. 4. From this figure we find that crack orientations are almost randomly distributed and 95% of 167 cracks are less than 1mm in length. In the later step these crack data are in use for calculating effective elastic moduli using crack model.

4. Measurement of Ultrasonic Wave Velocities

Ultrasonic wave velocity measurement is used to determine effective elastic moduli experimentally for the comparison with the values from the theoretical work. Ultrasonic wave velocities have been measured by many researchers for describing the anisotropic behavior of rock. They all agreed that ultrasonic wave velocity testing could be an appropriate way to assess the degree of crack propagation in rock.

As transverse isotropy is assumed, five independent measurements of ultrasonic wave velocity are required to determine five effective elastic moduli in experiment. The compliance matrix **C**, a relationship between stress and strain, is expressed in equation (13):

$$\begin{bmatrix}\sigma_x\\ \sigma_y\\ \sigma_z\\ \tau_{yz}\\ \tau_{zx}\\ \tau_{xy}\end{bmatrix}=\begin{bmatrix}C_{11}&C_{12}&C_{13}&0&0&0\\ C_{12}&C_{11}&C_{13}&0&0&0\\ C_{13}&C_{13}&C_{33}&0&0&0\\ 0&0&0&C_{44}&0&0\\ 0&0&0&0&C_{44}&0\\ 0&0&0&0&0&C_{66}\end{bmatrix}\begin{bmatrix}\varepsilon_x\\ \varepsilon_y\\ \varepsilon_z\\ \gamma_{yz}\\ \gamma_{zx}\\ \gamma_{xy}\end{bmatrix},\quad C_{66}=(C_{11}-C_{12})/2 \tag{13}$$

As noted earlier, Z is the axis of symmetry of transverse isotropy. The components of matrix C can be described as a function of ultrasonic wave velocities, as follows (Jones & Wang, 1981; Liao et al., 1997):

$$C_{11}=\rho V_{p,y}^2 \qquad C_{33}=\rho V_{p,z}^2$$

$$C_{44}=\rho V_{s,zx}^2 \qquad C_{66}=\rho V_{s,yx}^2$$

$$C_{13}=\sqrt{\left(2\rho V_{p,45}^2-\frac{C_{11}+C_{33}}{2}-C_{44}\right)-\frac{(C_{11}-C_{33})^2}{4}}-C_{44} \tag{14}$$

Where p = P (compressive) wave, s = S (shear) wave, y = wave direction : Y axis, z = wave direction : Z axis, yx = wave direction : Y axis and polarization : X axis on YX plane, zx = wave direction : Z axis and polarization : X axis on ZX plane, 45 = 45° angled direction on the YZ plane. For example, $V_{p,z}$ means P wave velocity measured in the direction of Z axis and $V_{s,zx}$ denotes S wave velocity measured in the direction of Z axis while

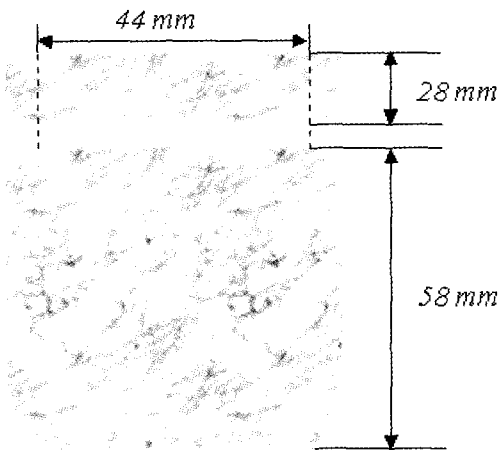

Fig. 5. Yeosan marble for the experiment.

S wave transducers are polarized in the direction of X axis. Using equation (14) and the inverse matrix of matrix C, we can obtain five effective elastic moduli experimentally.

Fig. 5 shows the experimental material, Yeosan marble. The shape of Yeosan marble is rectangular with 4 flat edges which make it possible to measure P wave velocity in the 45° angled direction on the YZ plane. Since the rock specimen is thin and the maximum principal stress is applied in the direction of Y axis, cracks are expected to grow in the direction of Y axis. Therefore, Z axis becomes the axis of symmetry of transverse isotropy.

There are several timing points which notify the arrival of P and S waves through the rock: The first arrival of the waves is defined as 'First Break' and the maximum position of the first arrived pulse is defined as 'First Peak'. First peak is used in our experiment because of easier measurement of elapsed time.

For more accurate measurement of wave arrival, two uniform samples (Aluminum alloy 6061-T6, Acryl) are used for zero calibration, which means the calibration for elapsed time when there is no specimen between two opposite transducers. When two kinds of uniform samples with two and four inches long are in use for measuring the elapsed time through the rock, results are shown in Fig. 6. In this figure, the time for zero calibration is derived when the length is zero. The values for P wave and S wave are 0.91 μsec and 0.73 μsec, respectively.

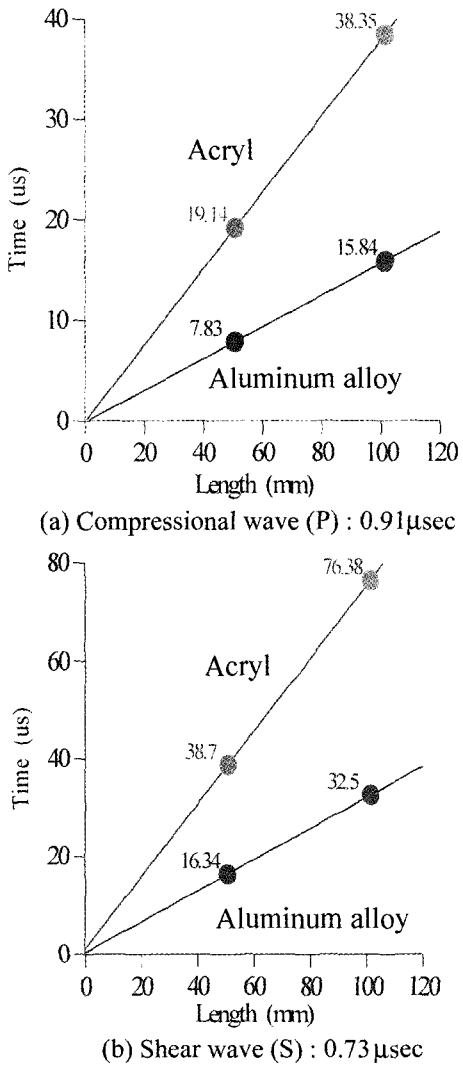

Fig. 6. Zero calibration using two uniform samples (Aluminum alloy 6061-T6, Acryl).

5. Results and Discussion

Effective elastic moduli can be determined from the theoretical basis using a crack model and from the experimental work using ultrasonic wave velocities. Then, we will compare these effective elastic moduli to validate the efficacy of crack model.

Liao *et al.* (1997) also measured ultrasonic wave velocities on a cylindrical rock specimen with and without a tensile load applied at the ends. They tried to determine five independent elastic constants from a transversely isotropic rock, argillite in the initial state.

However, the rock we use here is originally isotropic: rock can be assumed to be isotropic from wave velocities at different directions. This isotropic rock changes into transversely isotropic rock due to crack growth in rock. Despite the difference between two experiments, the axis of symmetry is in the same direction. The axis of symmetry is perpendicular to the loading direction, that is Y axis.

To satisfy the requirement that the axis of symmetry has to be perpendicular to the longitudinal axis, the shape of rock specimen is a thin rectangle as mentioned earlier in the previous part. This rock behaves like a transversely isotropic material after crack growth under the uniaxial compression.

First, we measured wave velocities during the uniaxial stress applied. Wave velocities increased at the early loading stage because open cracks in rock had closed. The crack model we use in this study does not describe the crack closure and the increase of elastic constants. Therefore, we measured wave velocities with zero load after loading an additional 1 ton at each stage. Fig. 7 shows the results of ultrasonic wave velocities.

From this figure, we can know that there is no region where velocity increases. Only region where velocity decreases exists because of crack growth after the 65% load of rock failure. P and S wave velocities in the direction of the axis of symmetry, Z axis decrease sharply because the cracks grow perpendicular to Z axis and they delay the arrival of waves, whereas P and S wave velocities in the isotropic planes parallel to XY plane decrease a little. The difference of wave velocities between different directions increases as the load increases, and consequently the degree of anisotropy increases.

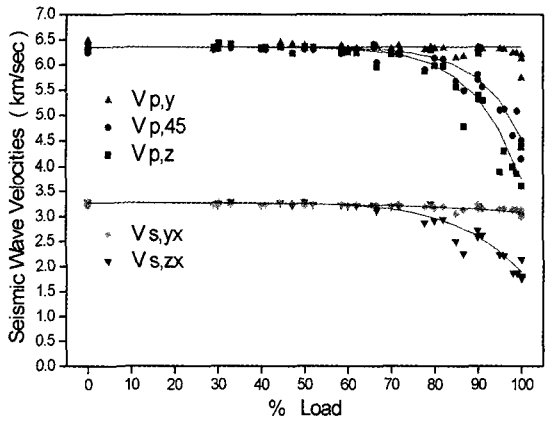

Fig. 7. Ultrasonic wave velocities as a function of load level (p = P (compressive) wave, s = S (shear) wave, y = wave direction : Y axis, z = wave direction : Z axis, yx = wave direction : Y axis and polarization : X axis on YX plane, zx = wave direction : Z axis and polarization : X axis on ZX plane, 45 = 45° angled direction on the YZ plane).

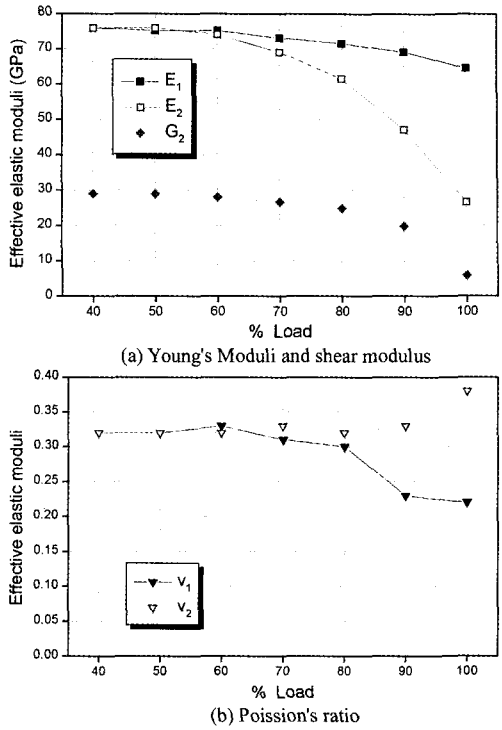

Fig. 8. Five effective elastic moduli determined from ultrasonic wave velocities.

From five wave velocities, five effective elastic moduli are calculated as shown in Fig. 8. E_1, ν_1 are elastic properties of isotropic planes, and E_2, ν_2, G_2 are elastic properties of planes that include the axis of symmetry. Though E_1 decreases smoothly as the load increases, E_2 decreases sharply. In Poissons ratio, ν_1 decreases in a small amount of value, whereas ν_2 increases.

We have determined five effective elastic moduli experimentally until now. These elastic moduli can also be determined theoretically as described earlier. We calculated the values numerically from the initial crack information that we observed using SEM. The number of cracks found on the area of 14.08 mm^2 was 167 and

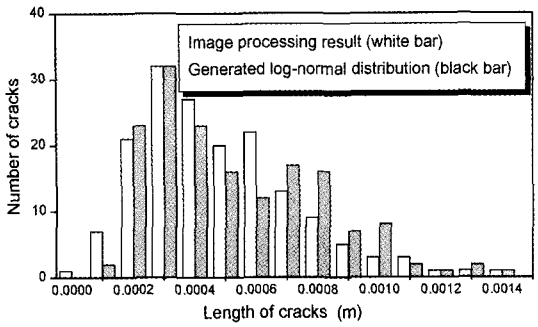

Fig. 9. Histogram of crack length.

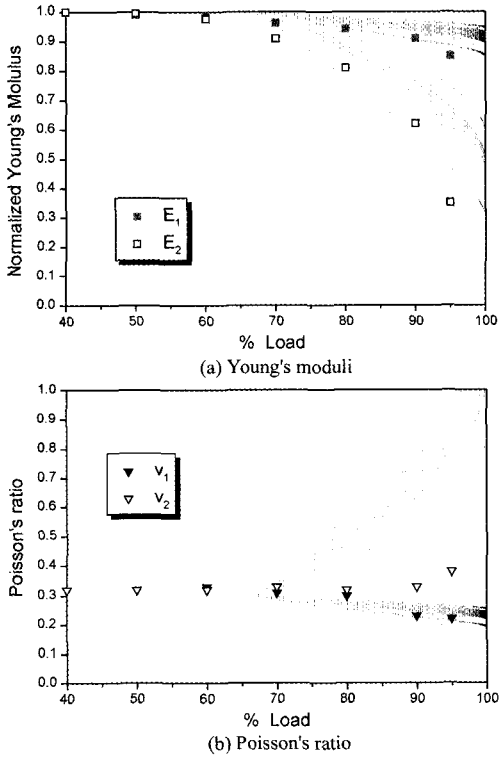

Fig. 10. Comparison of effective elastic moduli between theoretical and experimental methods.

crack orientation was uniformly distributed. The length of cracks is generated following log-normal distribution such as Fig. 9.

To compare the values from experimental and theoretical work, we normalized effective Youngs modulus with original value at zero load. Smaller dots in Fig. 10 indicate ten sets of effective elastic moduli calculated numerically and larger dots are values determined from ultrasonic wave velocity measurement. Crack model demonstrates well the increasing and decreasing tendencies in effective elastic moduli.

6. Conclusions

This study is focused on the validation of efficacy to predict the rock behavior under the uniaxial compression by using a mechanical crack model, that is, sliding crack model and by using ultrasonic wave velocities experimentally.

Due to crack growth which tends to be parallel to the loading direction, isotropic rock at the initial stage changes into transversely isotropic material. Non-linear behavior of transversely isotropic rock is described using five effective elastic moduli determined theoretically from crack model and experimentally from ultrasonic wave velocities. These two values show similar increasing and decreasing tendencies. E_1 decreases smoothly with crack growth, but E_2 and G_2 decrease sharply. ν_1 decreases as cracks grow while ν_2 increases.

If the initial crack information is acquired from such ways as direct measurement used in this study and scanline survey, the crack model can predict the non-linear behavior of rock successfully. In addition, this method can be applied to the coupled effect of rock.

Acknowledgements

Financial support for this research was provided by Seoul National University (서울대학교 발전기금 일반학술연구비, 연구관리번호: 98-09-2104).

References

1. Jeon, S., 1997, Development of a micromechanical crack model based on crack information: Environmental and safety concerns in underground construction, Proc. 1st Asian rock mech. Symp., 451-457.
2. Jones, L.E.A. & Wang, H.F., 1981, Ultrasonic velocities in cretaceous shales from the Williston basin: Geophys., 46, 288-297.
3. Kemeny, J.M. & Cook, N.G.W., 1987, Determination of rock fracture parameters from crack models for failure in compression: 28th US rock mech. Symp., 367-374.
4. Kemeny, J.M. & Cook, N.G.W., 1991, Micromechanics of deformation in rocks: Toughening mechanisms in quasi-brittle materials, 155-188.

5. Kemeny, J.M., 1993, The micromechanics of deformation and failure in rocks: Assessment and prevention of failure phenomena in rock engineering, Proc. Int. Symp., 23-33.
6. Kranz, R.L., 1983, Microcracks in rocks, A review: Tectonophysics, 100, 449-480.
7. Liao, J.J., Hu, T., & Chang, C., 1997, Determination of dynamic elastic constants of transversely isotropic rocks using a single cylinderical specimen: Int. j. rock mech. min. sci. & geomech. Abstr., 34. 7, 1045-1054.
8. Lockner, D.A., Walsh, J.B. & Byerlee, J.D., 1977, Changes in seismic velocity and attenuation during deformation of granite: J. geophys. Res., 82. 33, 5374-5378.
9. Reismann, H. & Pawlik, P.S., 1980, Elasticity - Theory and Application: John Wiley & Sons, 286-289.
10. Sayers, C.M., Van Munster J.G. & King, M.S., 1990, Stress-induced ultrasonic anisotropy in Berea sandstone: Int. j. rock mech. min. sci. & geomech. Abstr., 27. 5, 429-436.
11. Sayers, C.M. & Kachanov, M., 1995, Microcrack-induced elastic wave anisotropy of brittle rocks: J. geophys. Res., 100, 4149-4156.
12. Shea, V.R. & Hanson, D.R., 1988, Elastic wave velocity and attenuation as used to define phases of loading and failure in coal: Int. j. rock mech. min. sci. & geomech. Abstr., 25. 6, 431-437.
13. Sokolnikoff, I.S., 1956, Mathematical theory of elasticity: 2nd Ed., McGrow-Hill Book Com., Inc., 390-394.
14. Underwood, E.E., 1970, Quantitative stereology: Addison Wesley.
15. Watanabe, T. & Sassa, K., 1995, Velocity and amplitude of p-waves transmitted through fractured zones composed of multiple thin low-velocity layers: Int. j. rock mech. min. sci. & geomech. Abstr., 32. 4, 313-324.
16. Wu, B., King, M.S. & Hudson, J.A., 1991, Stress-induced ultrasonic wave velocity anisotropy in a sandstone: Int. j. rock mech. min. sci. & geomech. Abstr., 28. 1, 101-107.

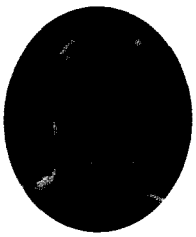

신 종 진

1998년 서울대학교 공과대학 자원공학과, 공학사
2000년 서울대학교 대학원 자원공학과, 공학석사

Tel : 017-356-2856
E-mail : sinzin@rockeng.snu.ac.kr
현재 미국 Stanford대학 유학중(박사과정)

전 석 원

1987년 서울대학교 공과대학 자원공학과, 공학사
1989년 서울대학교 대학원 자원공학과, 공학석사
1991년 미국 캘리포니아 주립대학, 공학석사
1996년 미국 아리조나 주립대학, 공학박사

Tel : 02-880-8807
E-mail : sjeon@rockeng.snu.ac.kr
현재 서울대학교 지구환경시스템공학부 교수